Fermi surfaces of tungsten silicide alloys

1990 J. Phys.: Condens. Matter 2 3747

(http://iopscience.iop.org/0953-8984/2/16/005)

J. Phys.: Condens. Matter 2 (1990) 3747-3758. Printed in the UK

Fermi surfaces of tungsten silicide alloys

Satoshi Itoh
Advanced Research Laboratory, Toshiba Research and Development Centre, Saiwaiku, Kawasakishi, Kanagawa 210, Japan

Received 11 September 1989, in final form 21 November 1989

Abstract. The Fermi surfaces of the tungsten silicide alloys WSi_2 and W_3Si, determined from semi-relativistic self-consistent band calculation, are presented. The former consists of simple closed sheets, while the latter is constructed from two closed sheets, two multiply connected surfaces and, possibly, one electron pocket. The Fermi levels of these silicides are located in the dip of the density of states. Additionally, the relationship between the content of tungsten atoms in the alloys and its electronic properties is discussed.

1. Introduction

In recent years, transition-metal silicides are finding increasingly important applications in silicon integrated-circuit technology as Schottky barriers, ohmic contacts, gate electrodes, low-resistivity interconnections and so on. Within this family of compounds, the refractory metal (e.g. vanadium, molybdenum and tungsten) silicides have attracted special attention, because of their high-temperature stability and their relatively low resistivity in comparison with doped polycrystalline silicon. Furthermore, these compounds are appropriate as interface diffusion barriers. Therefore, many experimental studies on various properties of the refractory metal silicides have been reported (see, e.g., Lau 1983).

Several crystal structures for the refractory metal silicides are obtained in equilibrium phase. For example, the phase diagram of tungsten silicide is shown in figure 1 (Massalski

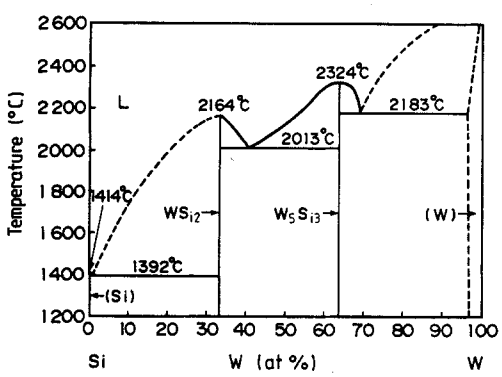

Figure 1. Phase diagram for the tungsten silicide system.

Table 1. Reported crystal structures for the tungsten silicides.

	Crystal structure	Lattice constant (au)
WSi_2	Tetragonal C11b	$a = 6.0698$
		$c = 14.891$
	Hexagonal C40	$a = 8.7192$
		$c = 12.121$
W_3Si_2	Tetragonal D8m	$a = 18.072$
		$c = 9.3384$
W_5Si_3	Hexagonal D8	$a = 13.587$
		$c = 9.1952$
	Tetragonal D8m	$a = 18.151$
		$c = 9.3806$
W_3Si	Cubic cP8	$a = 9.2786$

1986). In this phase diagram, WSi_2 and W_5Si_3 are shown as ordered alloys. Other crystal structures for the tungsten silicides were also reported (Dauben *et al* 1956, Matjusenko *et al* 1959, Matjusenko 1964, d'Heurle *et al* 1980). The reported crystal structures for the tungsten silicides are summarised in table 1.

Several theoretical attempts have been made to investigate the electronic structure of these materials. Recently, Bhattacharyya *et al* (1985) have carried out fully relativistic band calculations of $MoSi_2$ and WSi_2, using the norm-conserving pseudopotentials. They reported the band structures, decomposed densities of states (DOSs) and cohesive energies of $MoSi_2$ and WSi_2. Additionally, they found a large ionicity for both the molybdenum and the tungsten atoms. They also pointed out that the large ionicity is due to use of the basis functions which are rather delocalised spatially. Since the electronegativities of tungsten and silicon have nearly the same values, e.g. 1.6 and 1.7 for W and Si (Pauling 1960), respectively, there should be a small amount of charge transfer between refractory metal and silicon atoms in these compounds.

Although various ordered alloys in the tungsten silicides are known as presented in table 1, almost all experimental and theoretical studies are focused on WSi_x ($2.5 \geqslant x \geqslant 2$). However, it is necessary to promote a better understanding of the electronic properties of the tungsten silicides with various composition ratios, because of their enormous potential for future industrial applications. Therefore, in order to investigate the electronic properties of tungsten silicide ordered alloys thoroughly, we deal with the electronic structures of the most tungsten-rich and the most silicon-rich alloys, i.e. W_3Si and WSi_2. The electronic properties of alloys with other composition ratios may be inferred from the results obtained on W_3Si and WSi_2. Thus, the present paper will describe the electronic structures of the tungsten silicide alloys W_3Si and WSi_2 obtained from a semi-relativistic self-consistent band calculation in which the spin–orbit interaction is not taken into account. Since the structure of the Fermi surface profoundly influences the electronic properties of metals and metallic compounds, its bird's-eye view will be shown graphically. This paper is organised as follows. The computational details will be given in the next section. Section 3 contains numerical results. Finally, conclusions will be presented in the last section.

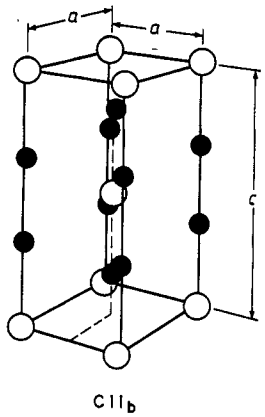

Figure 2. Body-centred tetragonal unit cell (C11b) of WSi_2: ○, tungsten atoms; ●, silicon atoms.

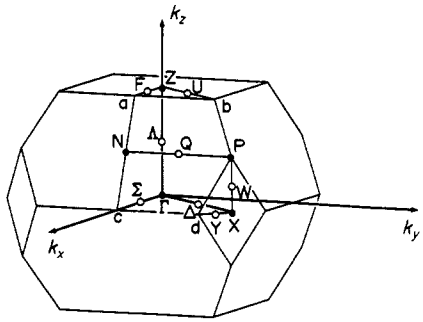

Figure 3. BZ corresponding to a body-centred tetragonal structure ($c > a$).

2. Crystal structures and computational details

The crystal structure of WSi_2 is shown in figure 2, in which each unit cell contains two molecules of WSi_2. Its Bravais lattice has body-centred tetragonal symmetry and the lattice parameters are $a = 6.0698$ au and $c = 14.8910$ au (Wyckoff 1963). The space group is I4/mmm. When silicon and tungsten atoms are regarded as hard spheres with the same radius, the packing fraction of that structure is about 0.7, which means that the structure is rather densely packed. The corresponding Brillouin zone (BZ) is shown in figure 3, where the symmetry points and lines are labelled in accordance with standard textbook practice (see, e.g., Bradley and Cracknell 1972).

On the other hand, the Bravais lattice of W_3Si is a simple cubic lattice with a lattice parameter of $a = 9.2786$ au (Pearson 1967). The space group is denoted by Pm3n, and its unit cell contains eight constituent atoms. The crystal structure of W_3Si is classified as A15 in the Strukurbericht notation (Pearson 1972). The packing fraction of the A15 structure is about 0.73. The crystal structure and its BZ are presented in figures 4 and 5, respectively.

Andersen (1975) proposed a highly efficient technique, called the linear muffin-tin orbitals (LMTO) atomic sphere approximation (ASA) method, for calculating the electronic structure in closely packed systems (i.e. metals and metallic compounds). Since the details of this method are described in pertinent literature (see, e.g., Skriver 1984, Andersen *et al* 1985), only a short review is given here. In the LMTO ASA method, the Wigner–Seitz cell is replaced by an overlapping atomic sphere with the same volume as the cell. The spherically symmetric potential, the so-called muffin-tin potential, can be defined inside each atomic sphere, so that the self-consistent potential extended over a whole system is constructed from the superposition of the muffin-tin potentials. The localised basis functions can be specified in the neighbourhood of each atomic sphere and are called the muffin-tin orbitals (MTOs). Therefore, the wavefunction can be constructed by a linear combination of the MTOs. Conditions for the wavefunction to be a solution of the Schrödinger equation for the whole system are as follows. In each atomic sphere, the sum of the MTOs coming from all other atomic spheres must interface with the MTOs centred at that atomic sphere in such a way that the resulting function is

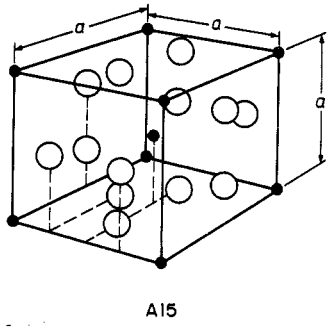

Figure 4. Cubic unit cell (A15) of W_3Si: ○, tungsten atoms; ●, silicon atoms.

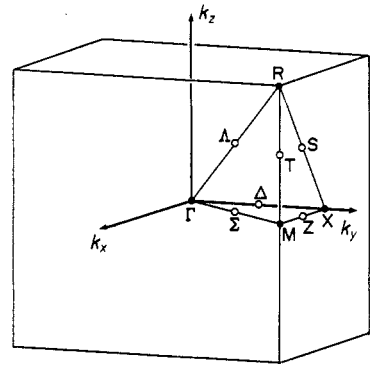

Figure 5. BZ corresponding to a simple cubic structure.

a solution of the Schrödinger equation within that atomic sphere. This condition gives a secular equation in the form of separate structure- and potential-dependent terms. The potential-dependent term can be linearised in the neighbourhood of an appropriate energy region. In other words, the energy-dependent wavefunctions are expanded with energy at an arbitrary value of energy. Then, non-linear terms are omitted.

In the present study, such a standard LMTO ASA method with the local density-functional approximation (Hohenberg and Kohn 1964) of the von Barth–Hedin (1972) exchange–correlation potential is used for the self-consistent calculation of the band structure, where the calculation includes all of the relativistic effects except the spin–orbit interaction.

In the LMTO ASA scheme, it is not at all required to set the radii of all atomic spheres to equal values, and to put the sphere only at atomic sites. By introducing empty spheres containing no atomic sites, highly reliable numerical results can be obtained using the LMTO ASA method even for loosely packed structures, such as semiconductors and insulators. As pointed out previously, however, the crystal structures for WSi_2 and W_3Si are rather dense, so that the conventional empty sphere is not needed. The contribution from the non-ASA to the overlap matrix, which is the so-called combined correction, is taken into account.

In the case of WSi_2, the distance between a W atom and its first-nearest neighbours is almost the same as that between a Si atom and its first-nearest atoms, so that the radius of atomic spheres centred at atomic positions is set to an equal value for W and Si atoms. On the other hand, in the case of W_3Si, the first interatomic distances of W–W, W–Si and Si–Si are $0.5a$, $0.5590a$ and $0.8660a$, respectively, where a is a lattice parameter of the unit cell. This fact suggests that the size of the atomic sphere centred at a W atom should be different from that for one centred at Si atom. The ratio of the atomic sphere radii centred at W and Si atoms was chosen as 0.8090. A larger atomic sphere was put at the Si atom site. It is important, in the LMTO ASA scheme, to choose the size of atomic spheres so as to reduce the degree of overlaps between any adjacent spheres.

For silicon and tungsten atoms, the core electron configurations are assigned as $1s^22s^22p^6$ and $1s^2 \ldots 4s^24p^64d^{10}4f^{14}5s^25p^6$, respectively. These core states are set to those in the free atoms. The core charge distributions are obtained from the solutions of the Dirac equation. That is, the so-called frozen-core approximation is adopted here. The valence electron configuration of silicon and tungsten atoms are $3s^23p^2$ and $5d^46s^2$,

respectively. The present calculation has been carried out by the s, p, d and f angular momentum basis set. Choosing 210 and 220 points of $\boldsymbol{k}$-vectors in the irreducible BZ for WSi_2 and W_3Si, the self-consistent band calculation has been carried out. In order to evaluate the DOS, the tetrahedron method (Lambin and Vigneron 1984) is used.

In the case of WSi_2, there are only three inequivalent atoms per unit cell, so that self-consistency was achieved successfully by iterative procedures, carried out several iteration times. On the other hand, inequivalent eight atoms are contained in the unit cell of W_3Si. For this reason, it is necessary to carry out the self-consistent iteration scheme carefully; the charge mixing ratio was typically 0.5% in the early stage of the iteration procedure, and more than 30 iteration loops were employed until self-consistency was fully achieved.

3. Results

Before discussing the numerical results obtained on the electronic structures of tungsten silicide alloys, the effect of the spin–orbit interaction on its Fermi surface structure was checked. Since tungsten is classified as a heavy atom, the spin–orbit interaction plays an important role in this system. In the atomic structure of tungsten, the spin–orbit splitting between valence electrons is of the order of 1 eV. There have been many experimental reports published on the Fermi surface of tungsten, based on the de Haas–van Alphen effect, anomalous skin effect, cyclotron resonance and so on, together with theoretical reports including non-relativistic and relativistic band calculations. This paper gives a short review of results of the non-relativistic and relativistic band calculations on tungsten in the BCC structure. The non-relativistic surface consists of four different sheets (Lomer 1962, 1964, Loucks 1965, Mattheiss 1965). Their main parts are described as an electron 'jack' centred at Γ and hole 'octahedra' at the symmetry point H. The others are smaller pieces; electron 'lenses' along Δ, and hole ellipsoids at N. The relativistic APW band calculation was originally carried out by Loucks (1966). The relativistic Fermi surface consists of two pieces: the electron jack at Γ and hole octahedra at H. Both the electron lenses and the hole ellipsoids at N have completely disappeared. The electron jack and hole octahedra no longer touch along the ΓH axis. In order to examine such relativistic effects on the Fermi surface of tungsten in the present calculation technique, a preliminary band calculation for BCC tungsten has been carried out. The resulting Fermi surface includes two main parts: the electron jack at Γ and hole octahedra at H. In addition, small ellipsoids are located at N. As expected, the absence of the spin–orbit interactions in the present calculation is shown by the absence of a gap between the electron jack and the hole octahedron along Δ. Since the spin–orbit interaction makes degenerate bands split, involving the interaction would slightly change the Fermi surface structure where the states are degenerate. From the present preliminary calculation for the Fermi surface of tungsten, the state density at the Fermi level is 0.381 states eV^{-1}/atom, which implies an electron specific heat of 2.15×10^{-4} cal mol^{-1} K^{-2} from elementary discussions. Its experimental value is $(2.5 \pm 1) \times 10^{-4}$ cal mol^{-1} K^{-2} (Hultgren *et al* 1963), so that the size of the calculated Fermi surface of tungsten is comparable with the experimental size. Therefore, by using the present semi-relativistic band calculation, it is expected to obtain the overall feature of the Fermi surface except for the Fermi surface with degenerate bands.

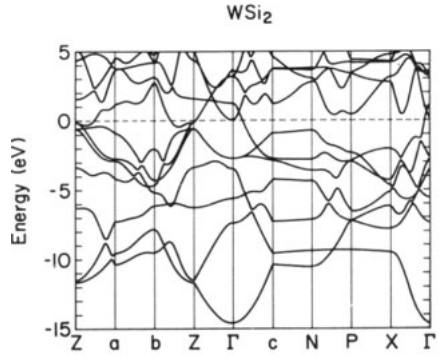

Figure 6. Self-consistent band structure for WSi_2. The energy is measured from the Fermi energy E_F.

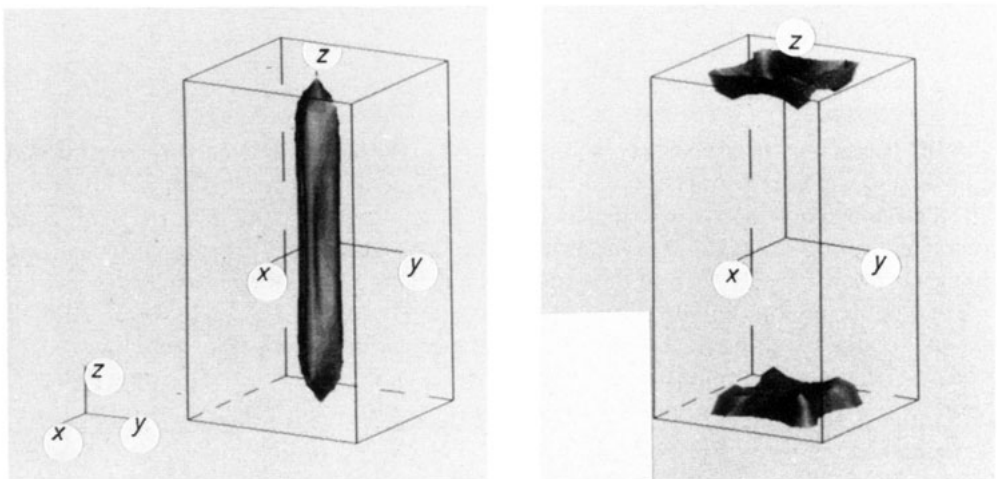

Figure 7. Fermi surface for WSi_2. The tetragonal cell does not directly correspond to the BZ for C11b.

Figure 6 shows the resulting self-consistent band structure of WSi_2, together with lines and points labelled as shown in the BZ for figure 3. The overall feature of the band structure is consistent with that calculated by Bhattacharyya *et al* (1985), based on the self-consistent relativistic pseudopotential scheme. It appears in figure 7 that the Fermi surface for WSi_2 consists of two bands: one is a hole surface surrounding Γ, and the other is an electron surface in the neighbourhood of Z. The former is constructed from the seventh band, and its shape is a constricted ellipsoid laid in the direction of z axis. The latter comes from the eighth band and has small horns. The hole ellipsoid touches the electron sheets along Λ, which is attributed to neglecting the spin–orbit interaction in the present semi-relativistic calculation. Therefore a small gap of the spin–orbit splitting between the ellipsoid and electron sheets is expected. In any case, the Fermi surface of WSi_2 is simple and has a small size. It seems that the electronic properties of WSi_2 have a semi-metallic character to some degree. For WSi_2, Martin *et al* (1984) observed a mixed conduction in which both holes and electrons participate. This experiment is not inconsistent with the results obtained from the present calculation.

The DOS is presented in figure 8, together with the decomposed DOSs on the basis of state density constituent atoms. The Fermi level is located in the dip of the DOS curve,

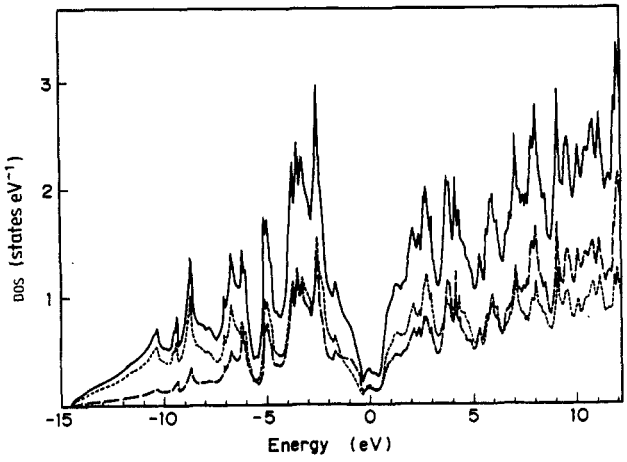

Figure 8. Total and decomposed DOSs for WSi_2: ———, total; — —, W; - - - -, Si. The energy is measured from the Fermi energy E_F.

Table 2. Gross charge distribution for WSi_2.

Atomic site	W	Si(1)	Si(2)
Gross population	5.5595	4.2204	4.2204

so that the state density at the Fermi level is rather small. This reduction in the DOS at the Fermi level contributes to stabilising its crystal structure and may cause a considerable reduction in its electronic conductivity. The DOS of the valence band consists of two parts: one is the DOS in the energy region from 0 to −7 eV and the other is the DOS below the energy of −7 eV. Referring to the decomposed DOSs, the origin of these structures can be explained. The lower-energy part of the valence band is mainly contributed from the s orbital of a silicon atom. Thus the band is almost the s band of a silicon atom. On the other hand, the upper part in the energy region from 0 to −7 eV consists mostly of p orbitals of the silicon atom and d orbitals of the tungsten atom, which implies a chemical bond between silicon and tungsten atoms. That is, the upper part of the valence band seems to come from the bonding state. The valence band contains a sharp peak structure at the energy of −2.5 eV, which is attributed mainly to the band degenerated doubly at Γ, i.e. the Γ^{5+} band.

By integrating the local DOS decomposed onto orbitals at each atom up to the Fermi energy, it is possible to estimate the charge density attributed to each atom. These values are shown in table 2. The atomic ionicities of silicon and tungsten are $+0.22e$ and $-0.44e$, respectively. A partial charge transfer from a tungsten site to a silicon site occurs. The present numerical result is consistent with the chemical trend in the electronegativities of silicon and tungsten (Pauling 1960).

It is possible to determine non-empirically the equilibrium atomic position from the result of the *ab initio* self-consistent band calculation. Since the space group I4/mmm of WSi_2 has a point group D_{4h} which contains only 16 symmetry operations, it is cumbersome to determine non-empirically the equilibrium position of all atoms. To avoid this cumbersomeness, we put the lattice parameter ratio c/a equal to the experimental value

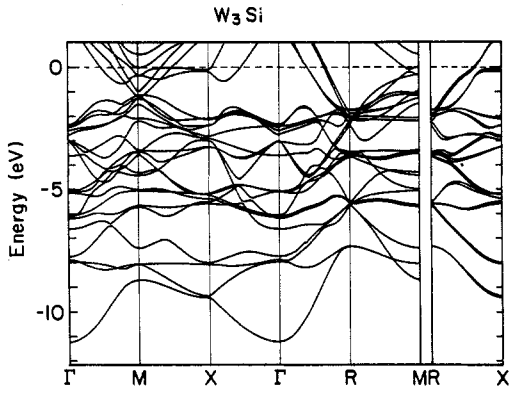

Figure 9. Self-consistent band structure for W_3Si. The energy is measured from the Fermi energy E_F.

(2.4533) and calculated the electronic structure at various values of the lattice parameter a. The resulting equilibrium lattice parameter is 6.103 au which is in good agreement with its observed values of 6.0698 au (Wyckoff 1963) within the error of 0.5%.

Figure 9 shows the band structure of W_3Si in a lower-energy region. The filled bands include broad low-lying bonding combinations of s–p states belonging to a Si atom that merges with the narrower d states of W atoms in the energy range 1–6 eV below the Fermi level. The lowest unoccupied states have a predominant d character, so that the Fermi level of W_3Si falls into the midst of the complex d band. This situation is very similar to that of another transition metal or refractory metal silicides (see, e.g., Mattheiss and Hensel 1989).

The Fermi surface of W_3Si (figure 10) is constructed from five bands, i.e. from the twenty-first to the twenty-fifth bands. The twenty-first band forms a simple hole surface enclosing Γ. The hole surface originating from the twenty-second band entirely contains that surface, and the closed sheet resembles an octahedron with knobs on its corners, which may be described as a 'hexacube' centred at Γ. The term 'hexacube' is named after the term 'tetracube' which was introduced originally by Andersen and Loucks (1968) in connection with the rare-earth Eu. The Fermi surfaces contributed from the twenty-third and twenty-fourth bands are multiply connected. Roughly speaking, these surfaces, particularly the surface from the twenty-third band, have simple round shapes and are sufficiently distorted from sphericity so as to touch the BZ boundary; the most likely boundary point is X. Finally, there are electron pockets at M which come from the twenty-fifth band. Since the size of the electron pockets, however, is very small, suffice it to say that the possibility of their existence is pointed out. The presence of the multiply connected Fermi surface (or open orbits), as is well known, implies characteristic transport properties such as non-saturation in the magnetoresistance, the Hall effect and thermoelectric power present. As far as the author knows, there have been no experimental reports on the Fermi surface topology of W_3Si heretofore. More extensive investigations on its Fermi surface structure are desired.

The total and decomposed DOSs are shown in figure 11 using the same method as that used for WSi_2. The DOS structure of W_3Si is similar to that of WSi_2; that is, the valence band consists largely of two parts, as mentioned previously. One is the lower band from -11 to -7 eV which corresponds to the s band. The other is the covalent-like bond formed between d orbitals of the tungsten atom and the p orbitals of the silicon atom. As expected from the calculated band structure, the Fermi level is positioned in the dip

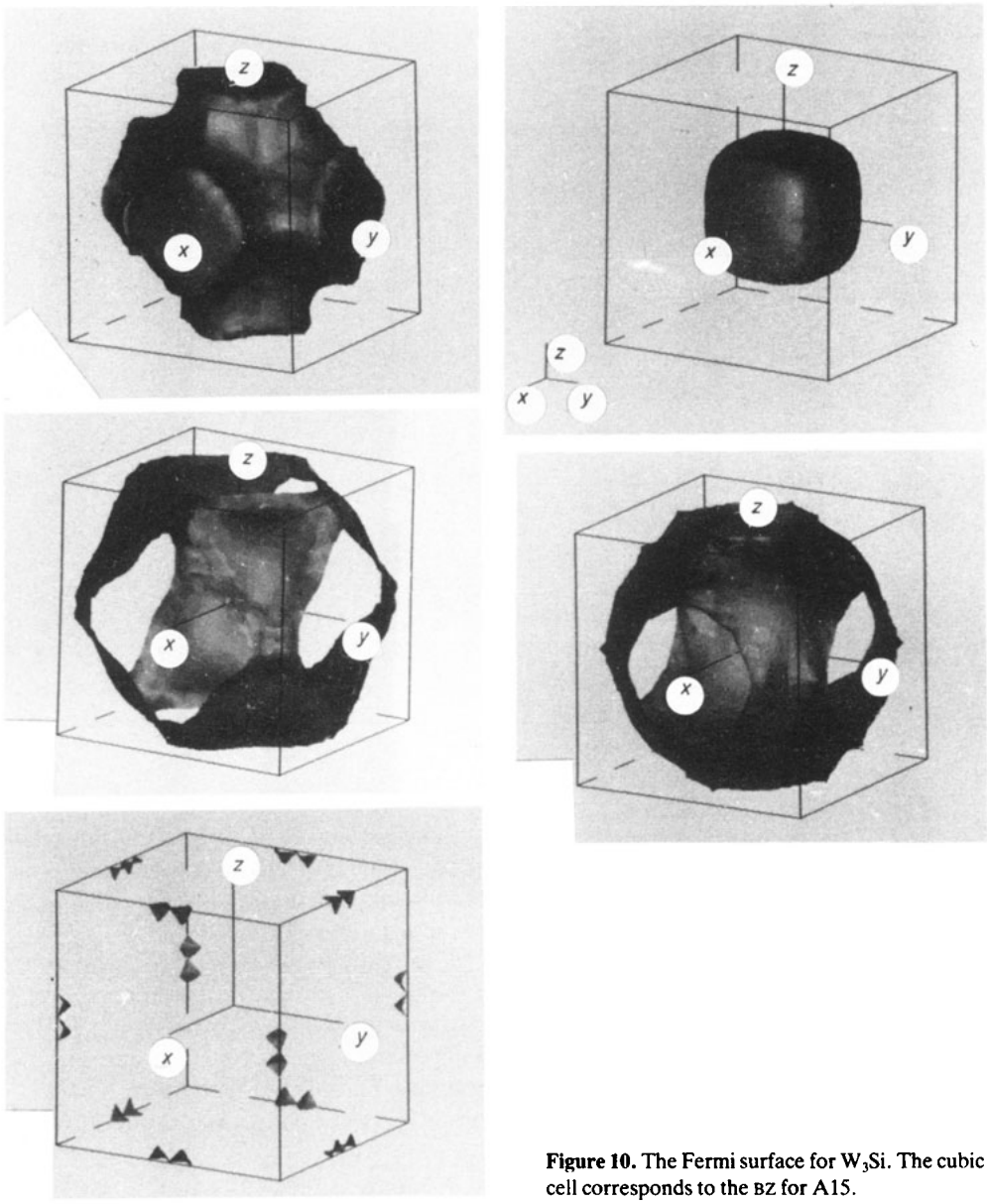

Figure 10. The Fermi surface for W_3Si. The cubic cell corresponds to the BZ for A15.

of the DOS, which causes a reduction in the state density at the Fermi level. A large amount of the reduction implies chemical bond formation between constituent atoms. That is, when the covalent bond is formed between constituent atoms, electronic states split into bonding and antibonding states. In a solid, these states are influenced by surrounding states and interact with each other. As a result, a continuous distribution of the energy levels (i.e. an energy band) appears. In the middle of the energy region between bonding and anti-bonding states, the DOS curve has a large dip. The tendency seen in the DOS structure of W_3Si seems to be the same as in the case of WSi_2.

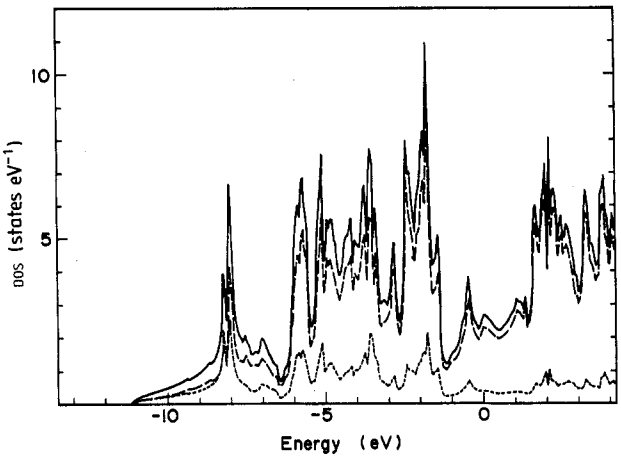

Figure 11. Total and decomposed DOSS for W_3Si: ———, total; ——, W; – – – –, Si. The energy is measured from the Fermi energy E_F.

Table 3. Gross charge distribution for W_3Si.

Atomic site	W(1)	W(2)	W(3)	W(4)	W(5)	W(6)	Si(1)	Si(2)
Gross population	5.581	5.539	5.647	5.581	5.539	5.647	5.242	5.221

Quantitatively, however, the state density at the Fermi level of W_3Si is considerably larger than that of WSi_2, so that W_3Si should have a higher electrical conductivity. This is merely a possibility, because the electronic conductivity of materials is determined by various processes in the electron scattering mechanism.

The electron population in W_3Si is obtained, using the same method for estimation that was used for WSi_2. The result is shown in table 3. The unit cell of W_3Si contains 44 valence electrons. Among them, the amount of valence electrons attributed to silicon atoms is 10.5*e*, and the remainder, 33.5*e*, is assigned to tungsten atoms. As a result, the silicon atoms are negatively charged to some degree. Partial charge transfer, however, seems to occur, and covalent-like bonds are formed between constituent atoms in W_3Si, similar to the case for WSi_2.

In order to determine equilibrium atomic positions in the unit cell, the electronic structure was calculated self-consistently at various values of the lattice parameters. The equilibrium lattice parameter obtained numerically is 9.298 au, which gives good agreement with the experimental value of 9.2786 au (Pearson 1967).

4. Conclusions

This paper has presented numerical results obtained for the semi-relativistic self-consistent band calculation for WSi_2 with the body-centred tetragonal structure (C11b) and for W_3Si with the simple cubic structure (A15). Both of the obtained band structures for WSi_2 and W_3Si show a more or less semi-metallic character, and these Fermi levels

fall into the dip of their DOS curves. In the case of WSi_2, the Fermi surface is constructed of two bands: one is a hole surface surrounding Γ, while the other is an electron surface in the neighbourhood of Z, which is compatible with the experimental results. On the other hand, the Fermi surface for W_3Si consists of five bands: two closed sheets which correspond to hole surfaces, two multiply connected surfaces and one electron pocket at M.

The electronic structures of WSi_2 and W_3Si ordered alloys have been theoretically presented. These correspond to the most silicon-rich and the most tungsten-rich alloys, respectively. In the intermediate composition ratio, ordered alloys W_3Si_2 and W_5Si_3 exist stably. In order to understand the electronic properties of tungsten silicide alloys, it might be required to investigate the electronic structures of W_3Si_2 and W_5Si_3. However, from the present calculation, it is possible to predict their electronic structures and to recognise the electronic character of tungsten silicide alloys. Although the band structures show specific characteristics in accordance with their crystal structure, the covalency of chemical bonds formed between tungsten and silicon atoms is of importance in these alloys. This fact causes its chemical stability and, perhaps, its high melting point. From the viewpoint of applications such as the fabrication of silicon integrated circuits, chemical stability is desirable, because of the requirement for high resistance to corrosion and degradation. When the silicide alloys are utilised as interconnection lines, it is also important that its electronic conductivity is high. From the result of the present calculation, it is expected that the tungsten-rich alloy has a lower resistivity and, as a result, the alloy containing a much higher number of tungsten atoms is advantageous for such an application. It has been reported that a thin film containing a large amount of tungsten atoms is likely to peel off after an annealing process (Bros *et al* 1983) in the fabrication of LSIs. The various condition parameters in the process technology may be optimised carefully. Moreover, since the Fermi surfaces for WSi_2 and W_3Si may not be obtained experimentally yet, such approaches, e.g. transverse magnetoresistance, de Haas–van Alphen effect and cyclotron resonance, are also required urgently.

Acknowledgments

I am grateful to Professor H L Skriver of the Technical University of Denmark for the use of his band calculation program. I also want to thank Mr T Kimura of Toshiba Corporation for assisting in the computer program development. I have benefited greatly from discussions with Professor T Fujiwara of the University of Tokyo. Special thanks are due to Mr M Azuma and Dr K Kato of Toshiba Corporation for continuous encouragement.

References

Andersen O K 1975 *Phys. Rev.* B **12** 3060

Andersen O K, Jepsen O and Glotzel D 1985 *Highlights of Condensed Matter Theory* ed F Bassani, F Fumi and M P Tosi (Amsterdam: North-Holland) p 59

Andersen O K and Loucks T L 1968 *Phys. Rev.* **167** 551

Bhattacharyya B K, Bylander D M and Kleinman L 1985 *Phys. Rev.* B **32** 7973

Bradley C J and Cracknell A P 1972 *The Mathematical Theory of Symmetry in Solids* (Oxford: Clarendon) p 105

Bros D L, Fair J A, Monnig K A and Saraswat K C 1983 *Solid State Technol.* **26** 183

Dauben C H, Templeton D H and Meyers C E 1956 *J. Phys. Chem.* **60** 443
d'Heurle F M, Petersson C S and Tsai M T 1980 *J. Appl. Phys.* **51** 5976
Hohenberg P and Kohn W 1964 *Phys. Rev.* **136** B864
Hultgren R R, Orr R L, Anderson P D and Kelly K K 1963 *Selected Values of Thermodynamic Properties of Metals and Alloys* (New York: Wiley) p 30
Lambin Ph and Vigneron J P 1984 *Phys. Rev.* B **29** 3430
Lau S S 1983 *VLSI Electronics: Microstructure Science* vol 6 (New York: Academic) p 329
Lomer W M 1962 *Proc. R. Soc.* **80** 489
—— 1964 *Proc. R. Soc.* **84** 327
Loucks T L 1965 *Phys. Rev.* **139** A1181
—— 1966 *Phys. Rev.* **143** 506
Martin T L, Malhotra V and Mahan J E 1984 *J. Electron. Mater.* **13** 309
Massalski T B 1986 *Binary Alloys Phase Diagrams* vol 2 (Metals Park, OH: Academic Society for Metals) p 2063
Matjusenko N N 1964 *Sov. Powder Metall. Met. Ceram.* **1** 15
Matjusenko N N, Efimenko L N and Solopikhin D P 1959 *Phys. Met. Metallogr. (USSR)* **8** 67
Mattheiss L F 1965 *Phys. Rev.* **139** A1893
Mattheiss L F and Hensel J C 1989 *Phys. Rev.* B **39** 7754
Pauling L 1960 *The Nature of the Chemical Bond* (Ithaca, NY: Cornell University Press)
Pearson W B 1967 *A Handbook of Lattice Spacings and Structures of Metals and Alloys* (Oxford: Pergamon) p 393
—— 1972 *The Crystal Chemistry and Physics of Metals and Alloys* (New York: Wiley) p 669
Skriver H L 1984 *The LMTO Method* (Berlin: Springer)
von Barth U and Hedin L 1972 *J. Phys. C: Solid State Phys.* **5** 1629
Wyckoff R W G 1963 *Crystal Structure* vol 1 (New York: Wiley) p 351